

# Accepted Manuscript

Synthesis and evaluation of a [<sup>18</sup>F]BODIPY-labeled Caspase-inhibitor

Christian Paul Ortmeier, Günter Haufe, Katrin Schwegmann, Sven Hermann, Michael Schäfers, Frederik Börgel, Bernhard Wunsch, Stefan Wagner, Verena Hugenberg

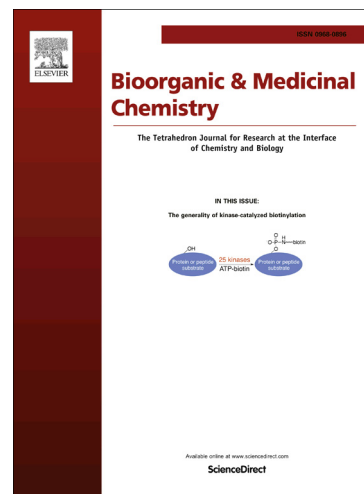
PII: S0968-0896(16)31490-0  
DOI: <http://dx.doi.org/10.1016/j.bmc.2017.02.033>  
Reference: BMC 13563

To appear in: *Bioorganic & Medicinal Chemistry*

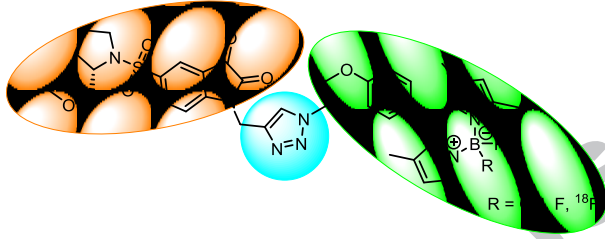
Received Date: 23 December 2016  
Revised Date: 11 February 2017  
Accepted Date: 14 February 2017

Please cite this article as: Ortmeier, C.P., Haufe, G., Schwegmann, K., Hermann, S., Schäfers, M., Börgel, F., Wunsch, B., Wagner, S., Hugenberg, V., Synthesis and evaluation of a [<sup>18</sup>F]BODIPY-labeled Caspase-inhibitor, *Bioorganic & Medicinal Chemistry* (2017), doi: <http://dx.doi.org/10.1016/j.bmc.2017.02.033>

This is a PDF file of an unedited manuscript that has been accepted for publication. As a service to our customers we are providing this early version of the manuscript. The manuscript will undergo copyediting, typesetting, and review of the resulting proof before it is published in its final form. Please note that during the production process errors may be discovered which could affect the content, and all legal disclaimers that apply to the journal pertain.



## Graphical Abstract.

<p><b>Synthesis and evaluation of a [<sup>18</sup>F]BODIPY-labeled Caspase-inhibitor</b></p> <p>Christian Paul Ortmeier, Günter Haufe,* Katrin Schwegmann, Sven Hermann, Michael Schäfers, Frederik Börgel, Bernhard Wunsch, Stefan Wagner, Verena Hugenberg*</p> <p><i>Departmental address here</i></p> 	<p>Leave this area blank for abstract info.</p>
--	---

## ARTICLE INFO

## ABSTRACT

*Article history:*

Received  
 Received in revised form  
 Accepted  
 Available online

*Keywords:*

BODIPY  
 Caspase inhibitor  
 Molecular imaging  
<sup>18</sup>F-labeling  
 Dual-function probe

BODIPYs (boron dipyrromethenes) are fluorescent dyes which show high stability and quantum yields. They feature the possibility of selective <sup>18</sup>F-fluorination at the boron-core. Attached to a bioactive molecule and labeled with [<sup>18</sup>F]fluorine, the resulting compounds are promising tracers for multimodal imaging *in vivo* and can be used for PET and fluorescence imaging. A BODIPY containing a phenyl and a hydroxy substituent on boron was synthesized and characterized. Fluorinated and hydroxy substituted dyes were coupled to an isatin-based caspase inhibitor *via* cycloaddition and the resulting compounds were evaluated *in vitro* in caspase inhibition assays. The metabolic stability and the formed metabolites were investigated by incubation with mouse liver microsomes and LC-MS analysis. Subsequently the fluorophores were labeled with [<sup>18</sup>F]fluorine and an *in vivo* biodistribution study using dynamic PET was performed.

2016 Elsevier Ltd. All rights reserved.


 Synthesis and evaluation of a [ $^{18}\text{F}$ ]BODIPY-labeled Caspase-inhibitor

 Christian Paul Ortmeyer<sup>a,b</sup>, Günter Haufe<sup>b,c,\*</sup>, Katrin Schwegmann<sup>d</sup>, Sven Hermann<sup>d</sup>, Michael Schäfers<sup>a,c,d</sup>,  
 Frederik Börgel<sup>e</sup>, Bernhard Wunsch<sup>e</sup>, Stefan Wagner<sup>a</sup>, Verena Hugenberg<sup>f,\*</sup>
<sup>a</sup>Department of Nuclear Medicine, University Hospital Münster, Albert-Schweitzer-Campus 1, Building A1, D-48149 Münster, Germany

<sup>b</sup>Organic Chemistry Institute, University of Münster, Corrensstr. 40, D-48149 Münster, Germany

<sup>c</sup>Cells-in-Motion Cluster of Excellence, University of Münster, Waldeyerstr. 15, D-48149 Münster, Germany

<sup>d</sup>European Institute for Molecular Imaging, University of Münster, Waldeyerstr. 15, D-48149 Münster, Germany

<sup>e</sup>Institute for Pharmaceutical and Medicinal Chemistry, University of Münster, Corrensstr. 48, D-48149 Münster, Germany

<sup>f</sup>Institute for Radiology, Nuclear Medicine and Molecular Imaging, HDZ NRW, Georgstr. 11, D-32545 Bad Oeynhausen, Germany

## ARTICLE INFO

## ABSTRACT

## Article history:

Received

Received in revised form

Accepted

Available online

## Keywords:

BODIPY

Caspase inhibitor

Molecular Imaging

 $^{18}\text{F}$ -labeling

Dual-labeled probe

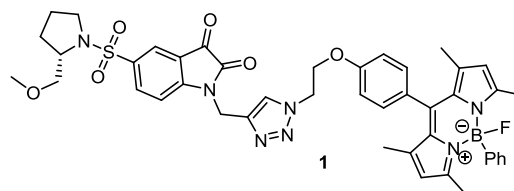
BODIPYs (boron dipyrromethenes) are fluorescent dyes which show high stability and quantum yields. They feature the possibility of selective  $^{18}\text{F}$ -fluorination at the boron-core. Attached to a bioactive molecule and labeled with [ $^{18}\text{F}$ ]fluorine, the resulting compounds are promising tracers for multimodal imaging *in vivo* and can be used for PET and fluorescence imaging. A BODIPY containing a phenyl and a hydroxy substituent on boron was synthesized and characterized. Fluorinated and hydroxy substituted dyes were coupled to an isatin-based caspase inhibitor *via* cycloaddition and the resulting compounds were evaluated *in vitro* in caspase inhibition assays. The metabolic stability and the formed metabolites were investigated by incubation with mouse liver microsomes and LC-MS analysis. Subsequently the fluorophores were labeled with [ $^{18}\text{F}$ ]fluorine and an *in vivo* biodistribution study using dynamic PET was performed.

2016 Elsevier Ltd. All rights reserved.

## 1. Introduction

Fluorescent probes based on boron dipyrromethene (BODIPYs) are a subject of numerous areas of research.<sup>1,2</sup> Their unique properties make them excellent fluorophores for a lot of different applications. Depending on the substituents on the ligand, BODIPYs usually possess high quantum yields,<sup>3</sup> variable Stokes shifts<sup>[1,4]</sup> and offer different synthetic pathways to influence the absorption and emission wavelength.<sup>5-7</sup> These comparatively apolar dyes often show high (photo)stability in a broad range of pH and polarity values as well as low toxicity. These features make them suitable for medicinal research and *in vivo* applications.<sup>8</sup> The main drawback is the often low solubility in water and physiological liquids. The implementations so far include chemo- and ionic sensors,<sup>9-17</sup> fluorescent switches,<sup>18-20</sup> laser dyes<sup>21-24</sup> as well as protein and DNA labeling.<sup>2,25-33</sup> Also the possibility to radiolabel these dyes with fluorine-18 to get dual-function probes has gained considerable interest.<sup>34-39</sup> Most recent publications using  $^{19}\text{F}/^{18}\text{F}$  isotopic exchange reactions or abstraction of one of the two fluorine atoms to yield radiolabeled BODIPYs suffer from low specific activity or unsuitable emission wavelengths for *in vivo* fluorescence imaging applications.

Herein we describe the synthesis of the first hydroxy- or monofluoro-substituted BODIPY with an azido group, its conjugation to an isatin-based caspase inhibitor to form compound **1** (Figure 1), and first proof-of-principle investigations with [ $^{18}\text{F}$ ]**1** as a dual-function probe for imaging.


 Figure 1. BODIPY-labeled caspase inhibitor **1**.

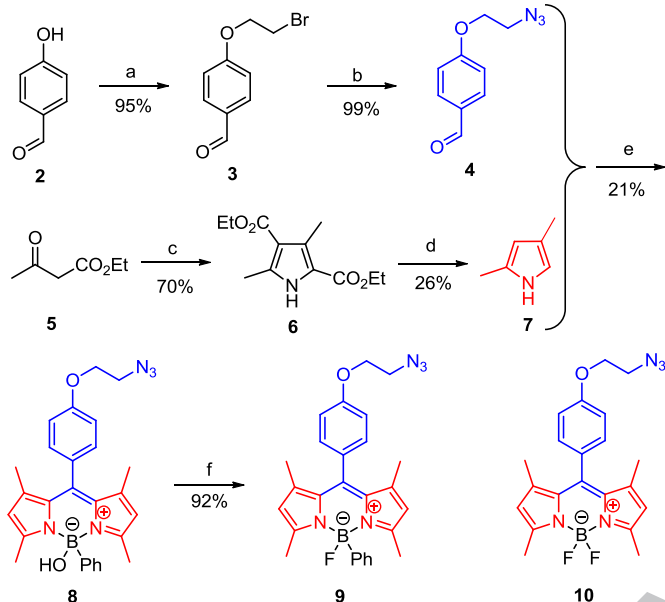
The enzyme family of caspases (cysteiny-l-aspartate-specific proteases) is crucial for the regulation of apoptotic processes within organisms.<sup>40</sup> Dysregulation of apoptosis, or programmed cell death, is related to many human diseases.<sup>41</sup> Therefore this group of enzymes represents an important target for *in vivo* imaging applications. Apart from other approaches, small molecules based on isatin have been extensively studied for *in vitro* and *in vivo* applications.<sup>42-51</sup> [ $^{18}\text{F}$ ]radiolabeling of isatins was already successful using different approaches.<sup>52-63</sup>

## 2. Results and discussion

## 2.1. Chemistry and radiochemistry

Synthesis of BODIPY **9** started from *p*-hydroxybenzaldehyde (**2**) by two substitution reactions *via* bromoethoxy compound **3** and 4-(2-azidoethoxy)-benzaldehyde (**4**) using literature-known procedures.<sup>64,65</sup> The second component, 2,4-dimethylpyrrole (**7**), was synthesized from ethyl acetoacetate (**5**) using Paal-Knorr pyrrole synthesis *via* the diester **6** followed by saponification and decarboxylation to **7**.<sup>66</sup> Aldehyde **4** and pyrrole **7** were then

condensed, complexed *in situ*<sup>1</sup> with dichlorophenylborane and hydrolyzed to obtain compound **8** in 21% yield. BODIPY **8** was fluorinated using potassium hydrogen fluoride to get fluorophore **9** in 92% yield. To obtain a high yield, activation using Lewis-acids (preferably trimethylsilyl trifluoromethanesulfonate) was necessary (Scheme 1). As an internal standard for the determination of the metabolic stability of **1**, a difluorinated BODIPY-derivative **10** was prepared utilizing a literature known procedure.<sup>65</sup>

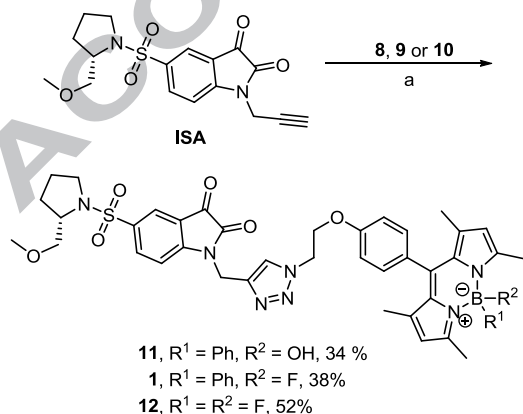


Reagents and conditions:

- (a) dibromoethane, CH<sub>3</sub>CN, K<sub>2</sub>CO<sub>3</sub>, RT, 24 h;  
 (b) NaN<sub>3</sub>, DMF, 140 °C, 1 h;  
 (c) 1. NaNO<sub>2</sub>, CH<sub>3</sub>COOH, 5 °C, 3 h, 2. Zn, 10 °C, 1 h, 3. 95 °C, 1 h;  
 (d) KOH, H<sub>2</sub>O, 140 °C, steam distillation  
 (e) 1. CF<sub>3</sub>COOH, CH<sub>2</sub>Cl<sub>2</sub>, RT, 12 h, 2. *p*-chloranil, CH<sub>2</sub>Cl<sub>2</sub>, RT, 15 min  
 3. NEt<sub>3</sub>, RT, 15 min, 4. PhBCl<sub>2</sub>, RT, 24 h, 5. H<sub>2</sub>O, RT, 1 h;  
 (f) TMSOTf, *t*-BuOH, KHF<sub>2</sub>, CH<sub>2</sub>Cl<sub>2</sub>, CH<sub>3</sub>CN, RT, 12 h.

**Scheme 1:** Synthesis of BODIPYs **8** and **9**.

From *N*-propargylisatin **ISA**<sup>43</sup> and the BODIPYs **8**, **9** and **10**, the fluorescent-labeled isatin derivative **11**, the target compound **1** and the reference compound **12** were prepared in copper-catalyzed [3+2]-cycloaddition reactions (“click reactions”) with yields of 34%, 38% and 52%, respectively (Scheme 2).



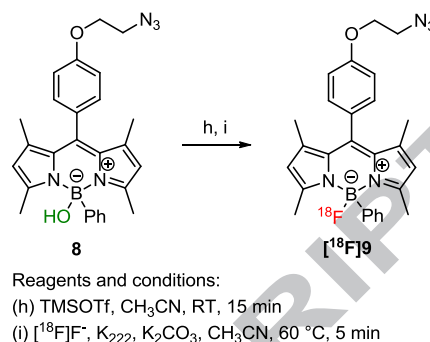
Reagents and conditions:

- (a) Sodium ascorbate, CuSO<sub>4</sub>, DMF, H<sub>2</sub>O, RT, 12 h

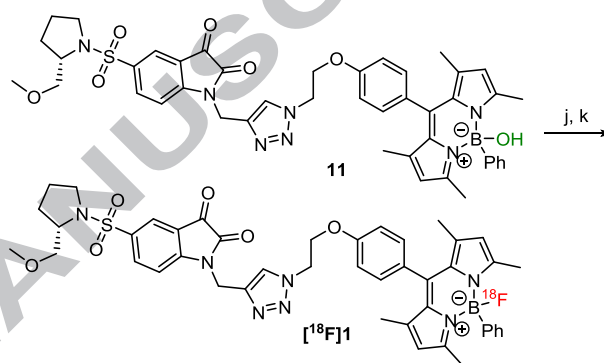
**Scheme 2:** Synthesis of labeled inhibitors **1**, **11** and **12**.

Bearing a phenyl and a hydroxy substituent on the boron atom, the fluorophore **8** and the fluorescent labeled isatin

derivative **11** were selectively labeled with [<sup>18</sup>F]fluoride in two steps applying a modified method of Hudnall *et al.*<sup>67</sup> under previously optimized conditions to form [<sup>18</sup>F]**9** and [<sup>18</sup>F]**1**, respectively (Schemes 3 and 4).



**Scheme 3:** Radiosynthesis of BODIPY [<sup>18</sup>F]**9**.



Reagents and conditions:

- (j) TMSOTf, CH<sub>3</sub>CN, RT, 15 min  
 (k) [<sup>18</sup>F]F<sup>-</sup>, K<sub>222</sub>, K<sub>2</sub>CO<sub>3</sub>, CH<sub>3</sub>CN, 60 °C, 10 min

**Scheme 4:** Radiosynthesis of dual-labeled probe [<sup>18</sup>F]**1**.

Compounds [<sup>18</sup>F]**9** and [<sup>18</sup>F]**1** were obtained in radiochemical yields of 21% ± 2% (n = 4) and 11% ± 6% (n = 4) with both high specific activity and radiochemical purity of 98% ± 2% (HPLC) and 97% ± 2% (HPLC), respectively. The experimental log*D* value (1.57) for [<sup>18</sup>F]**1** is considered as medium lipophilic. The compound is stable in human blood serum for at least 2 h. Unfortunately, the emission wavelength of **1** (λ<sub>max,em</sub> = 509 nm) is too short for fluorescence imaging *in vivo*. Currently, compounds with increased emission wavelengths are rationally designed and are under investigation.

## 2.2. In vitro inhibition assay

In order to evaluate the effects of labeling, compound **1** was compared with the lead compound **ISA**<sup>43</sup> using an *in vitro* caspase affinity test (see 4.4. *In vitro* enzyme inhibition assay). The results are summarized in Table 1.

**Table 1:** Caspase inhibition potencies (IC<sub>50</sub>-values) of the lead structure **ISA** and the probe **1** towards caspases-1, -3, -6, and -7.

compound	IC <sub>50</sub> (nM)			
	caspase-1	caspase-3	caspase-6	caspase-7
<b>ISA</b>	>50000	2.5 ± 1.5	>50000	10 ± 0.1
<b>1</b>	11800 ± 9600	34 ± 0.3	>50000	422 ± 8

The isatin **ISA** shows high selectivity towards caspase-3 and -7 with IC<sub>50</sub>-values in the nanomolar range. As expected, the labeling with a rather sterically demanding and lipophilic fluorophore BODIPY **9** resulting in inhibitor **1** led to an overall diminished activity of the tracer (see Table 1). Future experiments

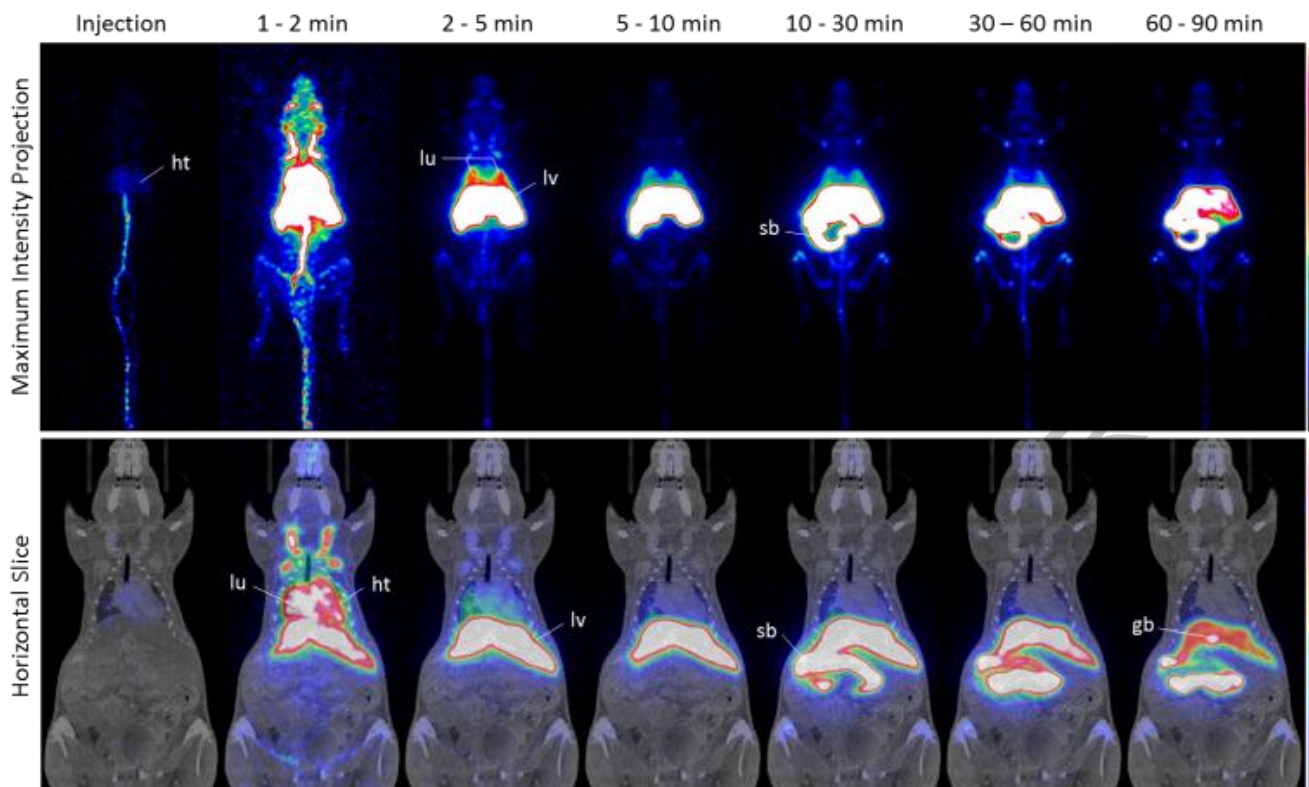


**Figure 2:** Distribution of radioactivity in an adult C57/B16 mouse after intravenous injection of  $[^{18}\text{F}]\mathbf{1}$  visualized by small-animal PET. Maximum intensity projections (MIP, upper row) of selected time frames display hepatobiliary excretion of  $[^{18}\text{F}]\mathbf{1}$ . Whole-body horizontal slices from fused PET/CT imaging (one selected slice, lower row) allow for better anatomical correlation and localization of radioactivity. Labeled structures are as follows: heart (ht), lung (lu), liver (lv), small bowel (sb), and gallbladder (gb).

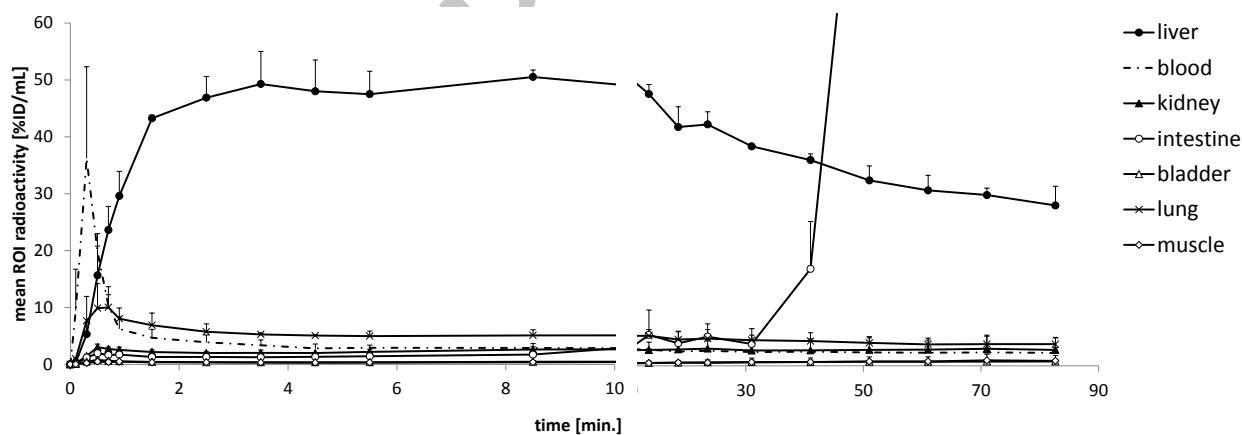


**Figure 3:** Time-activity concentration (TAC) curves illustrating the clearance of  $[^{18}\text{F}]\mathbf{1}$  from the blood due to hepatobiliary tracer elimination. Control ROI in reference tissues (lung, muscle) show low levels of radioactivity according to their blood fraction but no tracer accumulation.

will show, whether the effect of labeling is less pronounced, when spacer units are introduced between a bioactive moiety and the fluorophore.

### 2.3. *In vivo* biodistribution studies

After intravenous injection of ~10 MBq of [ $^{18}\text{F}$ ]1 an *in vivo* biodistribution study in adult C57/Bl6 mice was performed as a 90 min dynamic PET scan in combination with CT. Figure 2 shows representative maximum intensity projections (MIP) of whole body images at selected time points after tracer injection demonstrating notable and early accumulation of radioactivity in the liver followed by transport of radioactivity into the intestines. In contrast, no activity was observed in the kidneys and the urinary bladder reflecting that renal elimination of [ $^{18}\text{F}$ ]1 is negligible compared to hepatobiliary elimination of the tracer and/or potential metabolites. In the first minutes after injection, accumulation of radioactivity was observed in large vessels and well perfused tissues such as liver, lung, and heart followed by a continuously decreasing signal until the end of the study. Some uptake of radioactivity in bone was observed, which likely originates from free [ $^{18}\text{F}$ ]fluoride. Paulus *et al.* also observed for  $^{18}\text{F}$ -labelled BODIPYs an accumulation of radioactivity in bone, which might indicate insufficient metabolic stability of the boron-fluorine bond of the tracer *in vivo*.<sup>68</sup> In all *in vitro* tests the bond seemed to be stable. Selected ROIs were analysed quantitatively using PET image data (Figure 3).

Time curves of regional radioactivity concentrations expressed as percentage of injected dose per volume (% ID/mL) reveal a rapid washout of [ $^{18}\text{F}$ ]1 from blood. In fact, blood levels reach a peak 38 sec p.i. (36% ID/mL) with a subsequent decrease. [ $^{18}\text{F}$ ]1 is taken up by the liver rapidly with a peak at 8 min p.i. (50% ID/mL). Thereafter, a slow and steady decrease of radioactivity in the liver to 27% ID/mL at 90 min p.i. was observed. The kidneys present an uptake of radioactivity to a level of 3% ID/mL at 3 min p.i., which is maintained until the end of the imaging study. Concurrently, almost no radioactivity accumulated in the urinary bladder until 90 min p.i., excluding the renal route as an elimination pathway of [ $^{18}\text{F}$ ]1. Further regional analysis of brain, heart, spleen (data not shown), lung, and muscle tissue reveal a similar distribution kinetics. After the initial perfusion phase in the first 5 min the radioactivity concentration remains constant over 90 min.

After PET/CT imaging, mice were sacrificed, organs of interest were harvested, and the specific uptake of the tracer was determined by  $\gamma$ -counting, showing a similar distribution of the radioactivity as observed by TAC analysis (Figure 4)

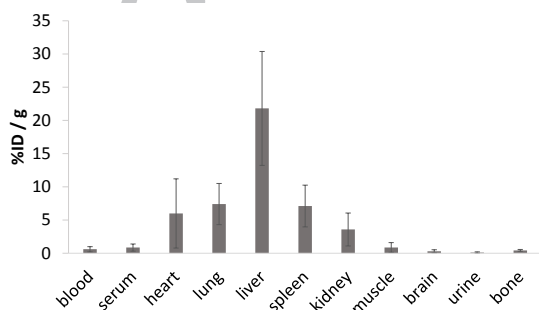


**Figure 4:** Quantitative *ex vivo* biodistribution data comparing radioactivity in various major organs at the termination time point, confirming the high uptake of [ $^{18}\text{F}$ ]1 in the liver found by PET *in vivo*.

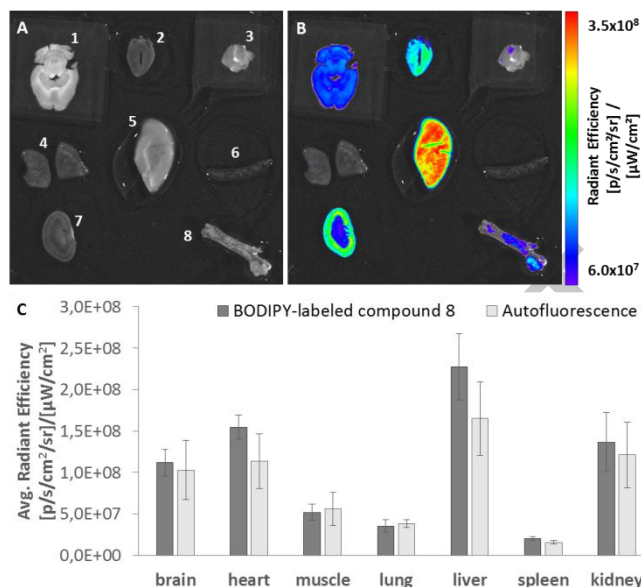


**Figure 5:** Representative FRI (fluorescence reflectance imaging) images of dissected organs (vibratome sections) of a C57/Bl6 mouse. Animals were sacrificed 2 h after intravenous injection of 2 nmol of **1** (A, white light image; B, FRI image overlay). C, Data of corresponding FRI measurements after injection of 2 nmol of **1** (dark grey bars) and untreated mice (light grey bars, autofluorescence). Compared to the autofluorescence signal fluorochrome accumulation was detected mainly in liver tissue. Lower to no intensity is found in muscle, lung, and spleen. (1 brain, 2 heart, 3 muscle, 4 lung, 5 liver, 6 spleen, 7 kidney, 8 femur).

Finally, we analyzed the biodistribution of the non-radioactive compound injected in healthy C57/Bl6 mice by measuring the fluorescence intensity in various organs. Figure 5 (A + B, white light and FRI image overlay) shows the tracer accumulation 2 hours after injection of 2 nmol per mouse. The highest uptake of the optical tracer compared to the autofluorescence signal of the organs was determined in liver tissue, indicating an elimination that was mainly driven by hepatic excretion in comparison to the lower uptake in the kidneys.

### 2.4. Determination of metabolic stability

In consideration of the predominant hepatobiliary elimination of **1**, a metabolism study using mouse liver microsomes was performed.<sup>69,70</sup> Compound **1** was incubated in a buffered suspension of mouse liver microsomes, NADPH/H<sup>+</sup> and UDPGA (UDP-activated glucuronic acid). The loss of tracer over time and the formation of possible metabolites were monitored by LC/MS. In order to investigate the stability in the presence of mouse liver microsomes, **1** was incubated for different periods of time using NADPH/H<sup>+</sup> as cofactor. The concentration of **1** was determined via external calibration using **12** as internal standard (ISTD). Compound **1** and the ISTD **12** were measured as formate adducts [M+HCOO]<sup>-</sup> in the negative scan mode.

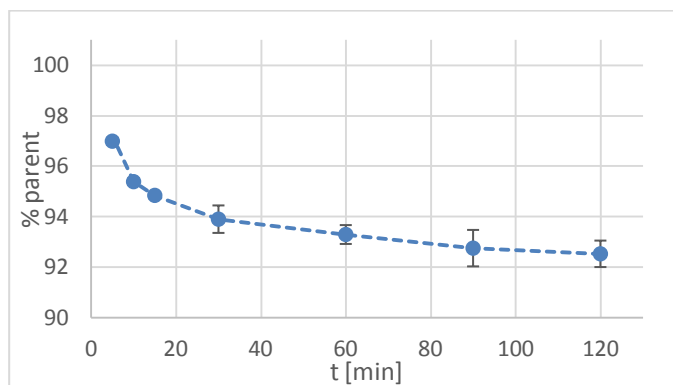
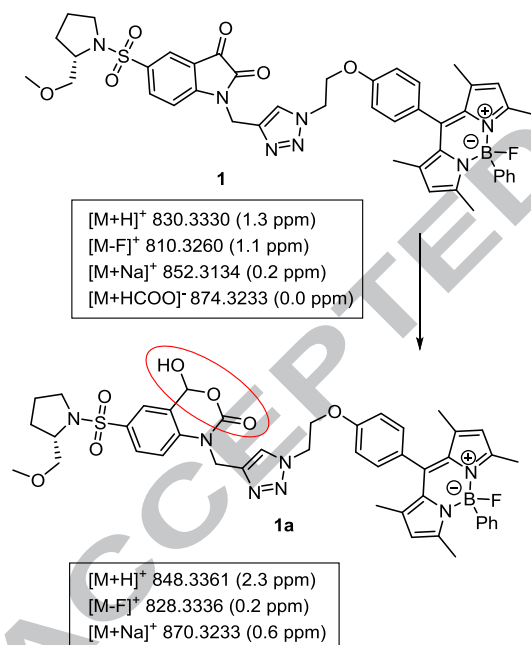


**Figure 6:** Degradation of **1** by mouse liver microsomes over time

Figure 6 shows the remaining parent compound **1** during incubation with mouse liver microsomes over a period of 120 min. This experiment indicates a high metabolic stability of **1**, since even after 120 min, more than 92% of **1** remained intact. For comparison and to prove the activity of the microsomes preparation, imipramine was incubated with the same materials. After 120 min only ~30% of the starting material was left confirming the high activity of the microsomes.

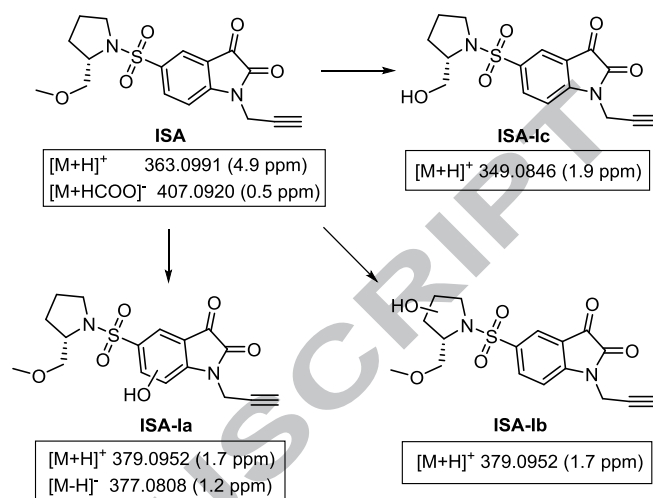
In order to analyze metabolites of **1**, LC was coupled with a quadrupole-time-of-flight-MS (qToF) system, which allowed identification and structure elucidation by analysis of the exact masses of metabolites and their fragments.



**Scheme 5:** Postulated metabolite **1a**.

After incubation of **1** with mouse liver microsomes, NADPH/H<sup>+</sup> and UDPGA only one metabolite **1a** could be detected by LC-MS (Scheme 5), which was also detected using only NADPH/H<sup>+</sup> as cofactor. Compared with the mass of **1**, the mass of the metabolite is higher by 18 (H<sub>2</sub>O), which should result from addition of H<sub>2</sub>O or oxidation (+O) and reduction (+2H). Scheme 5 shows the postulated structure of metabolite **1a**. This structure was postulated, as a similar metabolite was formed during electrochemical oxidation of similar isatins.<sup>[71]</sup> Furthermore, a metabolite with a mass higher by 16 (+O) or a metabolite with the mass higher by 2 (+2H) could not be detected. Due to low intensity of **1** and **1a** online dilution method was used to inject up to 100 μL of the sample, but the resulting intensities were still too low for fragmentation experiments.

Further metabolites with similar structures as those detected by Baumann *et al.* were not found for **1** in this study. In order to confirm these results, **ISA** was treated in the same way as **1** with mouse liver microsomes. The metabolites found for **ISA** are shown in Scheme 6.



**Scheme 6:** Detected metabolites of **ISA**.

Two monooxygenated metabolites **ISA-Ia** and **ISA-Ib** were identified. **ISA-Ia** was formed by hydroxylation of the benzene ring, since the ion [M-H]<sup>-</sup> was found in the negative scan mode. The second monooxygenated metabolite **ISA-Ib** resulted from oxidation of the pyrrolidine ring, as an ion [M-H]<sup>-</sup> was not found in the negative scan mode. Additionally, the O-demethylated metabolite **ISA-Ic** was observed. However, a metabolite correlating with the hemiacetal **1a** could not be detected.

### 3. Conclusions

The BODIPY derivatives **8** and **9** were prepared and used to label the isatin-based caspase inhibitor **ISA** to get compounds **11** and **1**. Both the fluorophore **8** and the labeled isatin **11** were <sup>18</sup>F-labeled in acceptable yields to get [<sup>18</sup>F]**9** as well as the dual-labeled probe [<sup>18</sup>F]**1**. An *in vitro* inhibition assay unveiled slightly altered selectivity and diminished inhibitory activity towards the target enzymes caspase-3 and caspase-7. First *in vivo* experiments using PET/CT and FRI led to the conclusion that the tracer is predominantly eliminated by a hepatobiliary pathway. However, incubation with mouse liver microsomes and NADPH/H<sup>+</sup> indicated a rather high metabolic stability. Our proof-of-principle investigation demonstrates the comparability of results from different imaging modalities using a BODIPY-based dual-labeled probe. In future work the fluorophores will be altered to emit light in the near infrared region, attain an increased water solubility and increase interaction with the target enzymes.

### 4. Experimental section

#### 4.1. General

All **chemicals** were purchased in highest quality and used without further purification. Dichloromethane for BODIPY-synthesis was dried over calcium hydride and was distilled freshly before use. Acetonitrile was dried over molecular sieves 3 Å. **Melting points** were determined with a Stuart SMP 3 (STUART SCIENTIFIC) and are uncorrected. <sup>1</sup>H, <sup>13</sup>C, <sup>11</sup>B and <sup>19</sup>F NMR spectra were measured on an AV400 (400 MHz) or an AV300 (300 MHz) spectrometer (BRUKER) using TMS or solvent signals as internal standard (<sup>1</sup>B NMR, 96.3 MHz, <sup>19</sup>F NMR, 282.4 MHz). **ESI-MS** spectra were recorded on a MicroToF Mass

spectrometer (BRUKER DALTONICS). **UV Spectra** were recorded on an U3010 Spectrometer (HITACHI). **Fluorescence spectra** were recorded on a F4500 Spectrometer (HITACHI). **Quantum yields** were determined in cooperation with the center for nanotechnology on a HAMAMATSU PHOTONICS absolute PL quantum yield measurement system (C9920-02), the software U6039-05 PLQY (HAMAMATSU PHOTONICS) was used for evaluation. **Gas chromatography/EI spectra** were recorded on a GC/MS QP2010 Series (SHIMADZU). Analytical and semi-preparative **HPLC** was conducted on two different systems:

- A. Two Smartline 1000 pumps (KNAUER), a Smartline 2500 UV-detector (KNAUER) and a GabiStar  $\gamma$ -detector (RAYTEST ISOTOPENMESSGERÄTE). A Nucleosil 100-5 C18 analytical column with the dimensions 4 mm x 250 mm was used.
- B. A K-500 and a K-501 pump (KNAUER), a K-2000 UV-detector (KNAUER) and a NaI(Tl) Scintibloc 51 SP51  $\gamma$ -detector (CHRISMATEC). A PHENOMENEX Gemini 5 $\mu$ m C18 column with the dimensions 10 mm x 250 mm was used.

The recorded data was processed by the GINA Star software. (RAYTEST ISOTOPENMESSGERÄTE).

**Column chromatography** was performed using either silica 60 (40-63  $\mu$ m, MERCK) or neutral Alumina (MP BIOMEDICALS GERMANY GMBH).

No carrier added [ $^{18}\text{F}$ ]fluoride was generated on a RDS111e cyclotron (CTI-SIEMENS) utilizing the  $^{18}\text{O}(\text{p},\text{n})^{18}\text{F}$  reaction using oxygen-18 enriched water and 10 MeV proton energy. **Radioisynthesis** was conducted on a TRACERLab Fx<sub>FDG</sub> synthesizer (GE HEALTHCARE). **Radiochemical yields** are based on the [ $^{18}\text{F}$ ]fluoride initial activity and are given decay corrected. **Radiochemical purity** is the ratio of the fraction of product radioactivity and total radioactivity and was determined by analytical HPLC. **Identification** of radioactive products was performed by co-injection of the non-radioactive reference compound. Only solvents of pharmaceutical purity from ABX and Milli-Q<sup>®</sup>-water or water for injection from B. BRAUN were used for radiosyntheses. Following a method described by Prante *et al.*,<sup>72</sup> the **distribution coefficient ( $\log D_{\text{exp}}$ )** of the radioactive compound was determined in a two-phase system consisting of 1-octanol and PBS-buffer (pH = 7.4) to determine the lipophilicity. For this purpose, the corresponding ligand (~20 kBq) was dissolved in buffer (500  $\mu$ L). 1-Octanol (500  $\mu$ L) was added and the mixture was shaken at room temperature for 1 min. To achieve phase separation, the system was centrifuged for 2 min at 3000 rpm. Subsequently a part of the octanol phase (400  $\mu$ L) was removed and buffer (400  $\mu$ L) was added. The combined phases were shaken and layers were separated according to the description above. Aliquots of the buffer and octanol layers (3  $\times$  100  $\mu$ L from every layer) were taken to measure radioactivity in a  $\gamma$ -counter. The measurement provided the activity in counts per minute (cpm), the values were decay corrected. By calculating the quotient of  $\frac{\text{cpm (1-Octanol)}}{\text{cpm (PBS)}}$  the  **$\log D_{\text{exp}}$**  can be determined as  $\log \frac{\text{cpm (1-Octanol)}}{\text{cpm (PBS)}}$ .

The **serum stability** of radioactive compounds was evaluated by incubation in human serum at 37 °C for up to 120 min. An aliquot of radioactive product (20  $\mu$ L, ~5 MBq) in PBS-buffer was added to a sample of human serum (200  $\mu$ L), and the mixture was incubated at 37 °C. Samples of 20  $\mu$ L each were taken after periods of 10, 30, 60, 90 and 120 min and quenched in MeOH/CH<sub>2</sub>Cl<sub>2</sub> (1:1 (v/v), 100  $\mu$ L) followed by centrifugation for 2 min. The clear solution was analyzed by analytical radio-HPLC system A.

## 4.2. Syntheses

### 4.2.1. 8-[4-(2-Azidoethoxy)phenyl]-4-hydroxy-4-phenyl-1,3,5,7-tetramethyl-4-bora-3a,4a-diaza-s-indacene (8)

2,4-Dimethylpyrrole (**7**) (0.861 mL, 8.4 mmol), 4-(2-azidoethoxy)benzaldehyde (**4**) (0.800 g, 4.2 mmol) and molecular sieve 3 $\text{\AA}$  (10 g) were added to carefully dried and degassed dichloromethane (250 mL) and trifluoroacetic acid (1 drop) was added. The mixture was stirred at RT for 12 h and then a solution of 2,3,5,6-tetrachloro-1,4-benzochinone (*p*-chloranil, 1.030 g, 4.2 mmol) in dichloromethane (200 mL) was added quickly. The deep-red suspension was stirred at RT for 15 min and triethylamine (2.32 mL, 16.8 mmol) was added dropwise. The mixture was stirred for additional 15 min before dichlorophenylborane (1.63 mL, 12.6 mmol) was added dropwise. After stirring for 24 h the mixture was filtered and water (150 mL) was added. The layers were separated and the organic layer was washed with water (3  $\times$  300 mL), dried over anhydrous sodium sulfate and solvents were removed under reduced pressure. The residue was dissolved in a minimum amount of trichloromethane and put on a small silica-pad. The pad was eluted quickly with trichloromethane to pre-purify the compound and to remove polymeric byproducts. The solvent was removed under reduced pressure and the residue was purified by column chromatography using neutral alumina (100 g, 6 cm  $\times$  7 cm, 35 mL fractions, cyclohexane/ethyl acetate, 1:1, v/v). All fluorescent fractions were combined, the solvents were removed under reduced pressure and the residue was dissolved in a minimum amount of dichloromethane. The solution was added dropwise to an excess of cooled *n*-pentane (100 mL, -15 °C) and the precipitate was filtered off and dried in vacuum to obtain the pure product as an orange solid. Yield: 0.408 g (21%) After this purification procedure, the product can be recrystallized from trichloromethane to obtain green-black, fluorescent crystals. Mp: complete decomposition starting at 137 °C. <sup>1</sup>H NMR (400 MHz, CDCl<sub>3</sub>):  $\delta$  = 1.45 (s, 6H, CH<sub>3</sub>), 2.19 (s, 6H, CH<sub>3</sub>), 3.67 (t, 2H, <sup>3</sup>J = 5.0 Hz, CH<sub>2</sub>N<sub>3</sub>), 4.22 (t, 2H, <sup>3</sup>J = 5.0 Hz, ArOCH<sub>2</sub>), 5.88 (s, 2H, Ar<sup>pyrrole</sup>CH), 7.03 – 7.10 (m, 2H, Ar-CH), 7.10-7.17 (m, 2H, Ar-CH), 7.18-7.24 (m, 2H, Ar-CH), 7.28-7.33 (m, 1H, Ar-CH), 7.37-7.44 (m, 2H, Ar-CH), B-OH not observed. <sup>13</sup>C NMR (100 MHz, CDCl<sub>3</sub>):  $\delta$  = 14.9, 15.4, 50.3, 67.1, 115.3, 121.2, 127.0, 128.5, 129.6, 129.8, 131.5, 132.1, 141.9, 155.6, 158.9. <sup>11</sup>B NMR (96 MHz, CDCl<sub>3</sub>):  $\delta$  = 1.20 (s). MS (ESI): Calculated for [C<sub>27</sub>H<sub>28</sub>BN<sub>5</sub>O<sub>2</sub>]Na<sup>+</sup>: 488.2228. Found: 488.2226. Calculated for 2[C<sub>27</sub>H<sub>28</sub>BN<sub>5</sub>O<sub>2</sub>]Na<sup>+</sup>: 953.4564. Found: 953.4573. UV:  $\lambda_{\text{max}}$ : 499 nm. FT:  $\lambda_{\text{max,emission}}$ : 509 nm. QY: 22%  $\pm$  0.5% (acetonitrile).

### 4.2.2. 8-[4-(2-Azidoethoxy)phenyl]-4-fluoro-4-phenyl-1,3,5,7-tetramethyl-4-bora-3a,4a-diaza-s-indacene (9)

A solution of trimethylsilyl trifluoromethanesulfonate in acetonitrile (0.25 M, 13.75 mL, 3.4 mmol) was added to a solution of compound **8** (80 mg, 0.2 mmol) in a mixture of acetonitrile and dichloromethane (2:1, v/v, 15 mL). After 15 min a solution of *tert*-butanol in acetonitrile (0.25 M, 13.75 mL, 3.4 mmol) was added at RT followed by solid potassium hydrogendifluoride (134 mg, 1.7 mmol). After stirring at RT for 12 h water (20 mL) was added and organic compounds were extracted with dichloromethane (3  $\times$  40 mL). The combined organic layers were dried over anhydrous sodium sulfate and solvents were removed under reduced pressure. The residue was purified by column chromatography with silica 60 (125 g, 13 cm  $\times$  5.5 cm, 50 mL fractions, cyclohexane/ethyl acetate, 2:1, v/v) to obtain the pure product as a red solid. Yield: 74 mg (92%). Mp: complete decomposition starting at 187 °C. <sup>1</sup>H NMR (400 MHz, CDCl<sub>3</sub>):  $\delta$  = 1.45 (s, 6H, CH<sub>3</sub>), 2.22 (s, 6H, CH<sub>3</sub>), 3.67 (t, 2H, <sup>3</sup>J = 5.0 Hz, CH<sub>2</sub>N<sub>3</sub>), 4.22 (t, 2H, <sup>3</sup>J = 5.0 Hz, ArOCH<sub>2</sub>), 5.88 (s,

2H, Ar<sup>pyrrole</sup>CH), 7.03 – 7.09 (m, 2H, Ar-CH), 7.10-7.17 (m, 2H, Ar-CH), 7.18-7.24 (m, 2H, Ar-CH), 7.28-7.33 (m, 1H, Ar-CH), 7.37-7.44 (m, 2H, Ar-CH). <sup>13</sup>C NMR (100 MHz, CDCl<sub>3</sub>): δ = 14.9, 15.4, 50.3, 67.1, 115.3, 121.2, 127.0, 128.5, 129.6, 129.8, 131.5, 132.1, 141.9, 155.6, 158.9. <sup>11</sup>B NMR (96 MHz, CDCl<sub>3</sub>): δ = 3.00 (s). <sup>19</sup>F NMR (282 MHz, CDCl<sub>3</sub>): δ = -173.92 (s). MS (ESI): Calculated for [C<sub>27</sub>H<sub>27</sub>BN<sub>5</sub>O<sub>7</sub>F]<sup>+</sup>H<sup>+</sup>: 468.2365. Found: 468.2376. Calculated for [C<sub>27</sub>H<sub>27</sub>BN<sub>5</sub>O<sub>7</sub>F]<sup>+</sup>Na<sup>+</sup>: 490.2185. Found: 490.2195. Calculated for 2[C<sub>27</sub>H<sub>27</sub>BN<sub>5</sub>O<sub>7</sub>F]<sup>+</sup>Na<sup>+</sup>: 957.4478. Found: 957.4497. UV: λ<sub>max</sub>: 500 nm. FT: λ<sub>max,emission</sub>: 509 nm. QY: 27% ± 0.5% (acetonitrile).

#### 4.2.3. General procedure A for copper-catalyzed [3+2]-cycloadditions (“Click-reaction”)

(S)-5-[(2-(Methoxymethyl)pyrrolidin-1-yl)sulfonyl]-1-(prop-2-yn-1-yl)indoline-2,3-dione (**ISA**) (86 mg, 0.236 mmol) and BODIPYs **8** or **9** were dissolved in dimethylformamide (40 mL) under an inert atmosphere. A suspension of a solution of copper(II)sulfate pentahydrate (429 mg, 1.72 mmol) in water (1.5 mL) and sodium ascorbate (426 mg, 2.15 mmol) in water (1.5 mL) was added after 5 min (suspension must be orange/white). After stirring at RT for 24 h dichloromethane (200 mL) was added. The organic layer was washed with water (4 × 100 mL), EDTA-solution (0.1 mol/L, 50 mL) and again with water (100 mL). The organic layer was dried over anhydrous sodium sulfate and solvents were removed under reduced pressure. The residue was purified by column chromatography with neutral Alumina (40 g, 12 cm × 2 cm, 10 mL fractions, cyclohexane/ethyl acetate, 1:1, v/v moving to pure ethyl acetate) to obtain compounds **11** or **1**, respectively.

##### 4.2.3.1. BODIPY-OH-labeled isatin **11**

Applying the general procedure (4.2.3) compound **8** (100 mg, 0.215 mmol) was transformed to compound **11**, which was obtained as an orange solid. Yield: 60 mg (34%). <sup>1</sup>H NMR (400 MHz, CDCl<sub>3</sub>): δ = 1.45 (s, 6H, Ar-CH<sub>3</sub>), 1.56-1.73 (m, 2H, pyrrolidineCH<sub>a</sub>), 1.80-1.94 (m, 2H, pyrrolidineCH<sub>b</sub>), 2.22 (s, 6H, Ar-CH<sub>3</sub>), 3.04-3.15 (m, 1H, pyrrolidineCH<sub>a</sub>), 3.34 (s, 3H, OCH<sub>3</sub>), 3.35 (dd, 1H, <sup>2</sup>J = 9.4 Hz, <sup>3</sup>J = 7.6 Hz, pyrrolidineCH<sub>a</sub>), 3.36-3.45 (m, 1H, pyrrolidineCH<sub>b</sub>), 3.56 (dd, 1H, <sup>2</sup>J = 9.4 Hz, <sup>3</sup>J = 3.8 Hz, pyrrolidineCH<sub>b</sub>), 3.68-3.77 (m, 1H, pyrrolidineCH), 4.42 (t, 2H, <sup>3</sup>J = 4.9 Hz, N<sup>triazole</sup>CH<sub>2</sub>), 4.79 (t, 2H, <sup>3</sup>J = 4.9 Hz, OCH<sub>2</sub>), 5.08 (s, 2H, N<sup>isatine</sup>CH<sub>2</sub>), 5.85 (s, 2H, Ar<sup>pyrrole</sup>CH), 6.94-7.03 (m, 2H, ArCH), 7.10-7.17 (m, 2H, ArCH), 7.18-7.24 (m, 2H, ArCH), 7.28-7.33 (m, 1H, ArCH), 7.37-7.44 (m, 2H, ArCH), 7.56 (d, 1H, <sup>3</sup>J = 8.3 Hz, Ar<sup>isatine</sup>CH), 7.92 (s, 1H, Ar<sup>triazole</sup>CH), 8.02 (d, 1H, <sup>4</sup>J = 1.8 Hz, Ar<sup>isatine</sup>CH), 8.09 (dd, 1H, <sup>3</sup>J = 8.3 Hz, <sup>4</sup>J = 1.8 Hz, Ar<sup>isatine</sup>CH). <sup>13</sup>C NMR (100 MHz, CDCl<sub>3</sub>): δ = 14.8, 15.6, 24.2, 28.9, 35.7, 49.4, 50.1, 59.2, 59.3, 66.2, 74.9, 112.1, 115.0, 117.4, 121.5, 124.6, 127.0, 129.4, 129.8, 130.0, 131.5, 132.0, 134.4, 137.7, 140.8, 141.3, 141.4, 153.0, 155.6, 157.7, 158.1, 181.8. <sup>11</sup>B NMR (96 MHz, CDCl<sub>3</sub>): δ = 1.17 (s). MS (ESI): Calculated for [C<sub>44</sub>H<sub>46</sub>BN<sub>7</sub>O<sub>7</sub>S]<sup>+</sup>Na<sup>+</sup>: 850.3165. Found: 850.3144. Calculated for [C<sub>44</sub>H<sub>46</sub>BN<sub>7</sub>O<sub>7</sub>SCH<sub>3</sub>OH]<sup>+</sup>Na<sup>+</sup>: 882.3427. Found: 882.3394. UV: λ<sub>max</sub>: 499 nm. FT: λ<sub>max,emission</sub>: 509 nm. QY: 6% ± 0.5% (acetonitrile).

##### 4.2.3.2. BODIPY-F-labeled isatin **1**

Applying the general procedure (4.2.3) compound **9** (98 mg, 0.210 mmol) was transformed to compound **1**, which was obtained as a red solid. Yield: 66 mg (38%). <sup>1</sup>H NMR (400 MHz, CDCl<sub>3</sub>): δ = 1.42 (s, 6H, Ar-CH<sub>3</sub>), 1.55-1.73 (m, 2H, pyrrolidineCH<sub>a</sub>), 1.81-1.93 (m, 2H, pyrrolidineCH<sub>b</sub>), 2.23 (s, 6H, Ar-CH<sub>3</sub>), 3.04-3.15 (m, 1H, pyrrolidineCH<sub>a</sub>), 3.34 (s, 3H, OCH<sub>3</sub>), 3.35 (dd, 1H, <sup>2</sup>J = 9.4 Hz, <sup>3</sup>J = 7.6 Hz, pyrrolidineCH<sub>a</sub>), 3.36-3.45 (m, 1H,

pyrrolidineCH<sub>b</sub>), 3.56 (dd, 1H, <sup>2</sup>J = 9.4 Hz, <sup>3</sup>J = 3.8 Hz, pyrrolidineCH<sub>b</sub>), 3.68-3.77 (m, 1H, pyrrolidineCH), 4.42 (t, 2H, <sup>3</sup>J = 4.9 Hz, N<sup>triazole</sup>CH<sub>2</sub>), 4.79 (t, 2H, <sup>3</sup>J = 4.9 Hz, OCH<sub>2</sub>), 5.08 (s, 2H, N<sup>isatine</sup>CH<sub>2</sub>), 5.85 (s, 2H, Ar<sup>pyrrole</sup>CH), 6.94 – 7.03 (m, 2H, ArCH), 7.10-7.17 (m, 2H, ArCH), 7.18-7.24 (m, 2H, ArCH), 7.28-7.33 (m, 1H, ArCH), 7.37-7.44 (m, 2H, ArCH), 7.56 (d, 1H, <sup>3</sup>J = 8.3 Hz, Ar<sup>isatine</sup>CH), 7.92 (s, 1H, Ar<sup>triazole</sup>CH), 8.02 (d, 1H, <sup>4</sup>J = 1.8 Hz, Ar<sup>isatine</sup>CH), 8.09 (dd, 1H, <sup>3</sup>J = 8.3 Hz, <sup>4</sup>J = 1.8 Hz, Ar<sup>isatine</sup>CH). <sup>13</sup>C NMR (100 MHz, CDCl<sub>3</sub>): δ = 14.8, 15.9, 24.2, 28.9, 35.7, 49.4, 50.1, 59.2, 59.3, 66.2, 74.9, 112.1, 115.0, 117.4, 121.5, 124.6, 127.0, 129.4, 129.8, 130.0, 131.5, 132.0, 134.4, 137.7, 140.8, 141.3, 141.4, 153.0, 155.6, 157.7, 158.1, 181.8. <sup>11</sup>B NMR (96 MHz, CDCl<sub>3</sub>): δ = 3.01 (s). <sup>19</sup>F NMR (282 MHz, CDCl<sub>3</sub>): δ = -173.86 (s). MS (ESI): Calculated for [C<sub>44</sub>H<sub>45</sub>BFN<sub>7</sub>O<sub>6</sub>S]<sup>+</sup>Na<sup>+</sup>: 852.3121. Found: 852.3137. Calculated for [C<sub>44</sub>H<sub>45</sub>BFN<sub>7</sub>O<sub>6</sub>SCH<sub>3</sub>OH]<sup>+</sup>Na<sup>+</sup>: 884.3383. Found: 884.3400. UV: λ<sub>max</sub>: 500 nm. FT: λ<sub>max,emission</sub>: 509 nm. QY: 12% ± 0.5% (acetonitrile).

#### 4.3. Radiosyntheses

##### 4.3.1. 8-[4-(2-Azidoethoxy)phenyl]-4-[<sup>18</sup>F]fluoro-4-phenyl-1,3,5,7-tetramethyl-4-bora-3a,4a-diaza-s-indacene ([<sup>18</sup>F]**9**)

A solution of compound **8** (580 μg, 1.25 μmol) was dissolved in acetonitrile (400 μL) and trimethylsilyl trifluoromethanesulfonate (5.5 μL, 30 μmol, 24 equiv) was added. The solution was shaken at RT for 15 min and added to previously dried [<sup>18</sup>F]fluoride (540–4924 MBq) in a TRACERLab Fx<sub>FDG</sub> synthesizer. The mixture was stirred for 5 min at 60 °C and purified on HPLC-system B using a PHENOMENEX Gemini 5 μm C18 column (R<sub>t</sub>: 19.8 min). The product was obtained in radiochemical yields (rcy) of 21% ± 2.2% (d.c.) in 84 ± 13 min (n = 4). To verify high purity, the isolated compound [<sup>18</sup>F]**9** was injected to analytical HPLC-system A (R<sub>t</sub> = 8.9 min). The gradient was 10% to 90% CH<sub>3</sub>CN in water (0.1% TFA) over 9 min, followed by a linear gradient from 90% to 10% CH<sub>3</sub>CN in water (0.1% TFA) over 6 min with λ = 254 nm and a flow rate of 1 mL·min<sup>-1</sup>. The radiochemical purity was determined to be > 98% in all cases. To exclude the possibility of [<sup>18</sup>F]fluoride contamination, additional TLC quality control (QC) was performed (see SI). Usually to determine the specific activity (A<sub>S</sub>) of a radiolabeled compound a UV calibration curve of the corresponding non-radioactive isotopomer is generated with defined concentrations using analytical radio-HPLC. Then the concentration can be calculated after HPLC quality control using the solution of the radiolabeled compound, which also contains the corresponding carrier (the <sup>19</sup>F-counterpart). With a known concentration the A<sub>S</sub> can be determined. In the case of compound [<sup>18</sup>F]**9** the corresponding isotopomer **9** showed a detection limit of 0.8 μg/mL in the UV-channel. Since UV-signals belonging to **9** were not occurring during QC of the final preparation of [<sup>18</sup>F]**9**, the A<sub>S</sub> was calculated to ≥ 514 GBq/μmol using the concentration of the detection limit.

##### 4.3.2. BODIPY-<sup>18</sup>F-labeled isatin ([<sup>18</sup>F]**1**)

A solution of compound **11** (490 μg, 0.59 μmol) was dissolved in acetonitrile (400 μL) and trimethylsilyl trifluoromethanesulfonate (5.5 μL, 30 μmol, 51 equiv) was added. The solution was shaken at RT for 15 min and added to previously dried [<sup>18</sup>F]fluoride (366–4835 MBq) in the automated synthesizer. The mixture was stirred for 10 min at 60 °C and purified on HPLC-System B using the a ACE 5 AQ column (R<sub>t</sub>: 17.8 min). The product was obtained in radiochemical yields (rcy) of 11% ± 6.1% (d.c.) in 91 ± 6 min (n = 4). To verify high purity the isolated compound [<sup>18</sup>F]**1** was injected to analytical

HPLC-system A ( $R_t = 12.0$  min). The gradient was 10% to 90%  $\text{CH}_3\text{CN}$  in water (0.1% TFA) over 9 min, followed by a linear gradient from 90% to 10%  $\text{CH}_3\text{CN}$  in water (0.1% TFA) over 6 min with  $\lambda = 254$  nm and a flow rate of  $1 \text{ mL}\cdot\text{min}^{-1}$ . The radiochemical purity was determined to be  $97\% \pm 2\%$ . To exclude the possibility of [ $^{18}\text{F}$ ]fluoride contamination, additional TLC quality control was performed (see SI). The test of serum stability was also performed on this system. In human blood serum [ $^{18}\text{F}$ ]**1** was stable for at least 120 min at  $37^\circ\text{C}$ . The  $\log D_{\text{exp}}$  value was determined to be 1.57. Specific activity had to be calculated similar to preparations of [ $^{18}\text{F}$ ]**9** due to concentrations below the detection limit. In the case of compound [ $^{18}\text{F}$ ]**1** the corresponding isotopomer **1** showed a detection limit of  $0.8 \mu\text{g}/\text{mL}$  in the UV-channel at different wavelengths. Since UV-signals belonging to **1** were not occurring during QC of the final preparation of [ $^{18}\text{F}$ ]**1**, the  $A_S$  was calculated to  $\geq 166 \text{ GBq}/\mu\text{mol}$  using the concentration of the detection limit.

#### 4.4. *In vitro* enzyme inhibition assay

An *in vitro* inhibition assay was performed to determine the effect of the BODIPY-labeling on both inhibition potency and selectivity. The inhibitory activity of the lead compound **ISA** and compound **1** was evaluated as  $\text{IC}_{50}$  values towards caspases-1, -3, -6, and -7. Recombinant human caspases and their substrates were purchased from ALEXIS BIOMEDICALS (Switzerland). As described previously,<sup>47</sup> reaction rates showing the inhibitory activity were determined by measuring the accumulation of the cleaved fluorogenic product AMC (7-amino-4-methylcoumarin) with a TriStar<sup>2</sup> Multimode Reader (BERTHOLD TECHNOLOGIES) at excitation and emission wavelengths of 360 and 460 nm, respectively. All assays were performed in a volume of  $200 \mu\text{L}$  at  $37^\circ\text{C}$  in reaction buffer containing the non-radioactive compounds in DMSO each in single doses ( $500 \mu\text{M}$ ,  $50 \mu\text{M}$ ,  $5 \mu\text{M}$ ,  $500 \text{ nM}$ ,  $50 \text{ nM}$ ,  $5 \text{ nM}$ ,  $500 \text{ pM}$ ,  $50 \text{ pM}$ , or  $5 \text{ pM}$ ). Recombinant caspases were diluted into the appropriate buffer to a concentration of 0.5 units per assay (=  $500 \text{ pmol}$  substrate conversion after 60 min). After incubation for 10 min, the peptide substrate ( $10 \mu\text{M}$ ) was added and reacted for further 10 min. The  $\text{IC}_{50}$  values were determined by nonlinear regression analysis using the XMGRACE program (Linux software).

#### 4.5. Animals

Eleven- to fourteen-week-old C57/BL6 mice (21-30 g body weight) were used for all experiments. Animal studies were approved by the office for environment, nature and municipal affairs of the land of North Rhine-Westphalia, Germany.

#### 4.6. Small Animal PET/CT Scanning

For PET/CT studies anaesthesia was induced by placing the mice ( $n = 3$ ) in an anaesthesia induction chamber filled with 3% isoflurane in air until the animal was completely anaesthetized. Then, the mice were transferred to a heated PET scanner bed, isoflurane anaesthesia was maintained (1.5 - 2% in oxygen) and biosignals (respiration, ECG, body temperature) were monitored. A catheter (27G diameter) was placed in one of the tail veins, flushed with saline ( $50 \mu\text{L}$ ) and connected to the injection line. In order to prevent the eyes of running dry they were moistened with eye salve. The setup for radiotracer injection consists of a tail vein catheter, a  $100 \mu\text{L}$  reservoir filled with the radiotracer [ $^{18}\text{F}$ ]**1** ( $9.2\text{-}9.9 \text{ MBq}$ ) and an injection pump holding a syringe filled with saline. For PET imaging (32 module quadHIDAC, Oxford Positron Systems Ltd., Oxford, UK) the scanner bed was automatically positioned in the centre of the camera field-of-view and PET list mode acquisition was started. Simultaneously the radiotracer reservoir was injected into the mouse by an injection

pump controlled saline flush ( $300 \mu\text{L}/\text{min}$ ). After 90 min of PET scanning, the scanning bed was transferred to the computed tomography (CT) scanner (Inveon, Siemens Medical Solutions, U.S.) and a CT acquisition with a spatial resolution of  $80 \mu\text{m}$  was performed for each mouse. Reconstructed image data sets were co-registered based on extrinsic markers attached to the multimodal scanning bed and the in-house developed image analysis software MEDgical. Three-dimensional volumes of interest (VOIs) were defined over the respective organs in CT data sets, transferred to the co-registered PET data and analyzed quantitatively. Regional uptake was calculated as percentage of injected dose by dividing counts per milliliter in the ROI by total counts in the mouse multiplied by 100 (% ID/mL).

After PET imaging, mice were sacrificed by cervical dislocation and organs of interest were harvested, weighted and counted using a Wizard<sup>2</sup> automatic  $\gamma$ -counter (PERKIN ELMER). The percentage of tracer uptake stated as percentage injected dose per gram of tissue (% ID/g) was calculated as the activity bound to tissue per actual injected dose per organ weight, decay-corrected to the start time of counting.

#### 4.7. Fluorescence reflectance imaging (FRI)

For Fluorescence Reflectance Imaging (FRI) mice were anesthetized by isoflurane/ $\text{O}_2$ , and the BODIPY-labeled compound **1** ( $2 \text{ nmol}$ ) was injected into the tail vein. Two hours after injection mice ( $n = 3$ ) were sacrificed and organs were rapidly removed and cut on a Vibrating Blade Microtome VT1200S (LEICA) at  $500 \mu\text{m}$  thickness and placed on a petri dish. FRI was performed using the IVIS Spectrum small-animal imaging system (PERKIN ELMER). Excitation was achieved at  $465 \text{ nm}$ , and emitted light was filtered by a bandpass filter ( $540 \text{ nm}$ ). The following settings were chosen: binning: 1, f-stop: 2, field of view: B ( $6.6 \text{ cm}$ ), exposure time:  $120 \text{ sec}$ . Images were analyzed with the software Living Image 4.2.0 (PERKIN ELMER). Grayscale photographic images and fluorescence color images were superimposed. Regions of interest (ROIs) were drawn over the tissue samples using the photographic images. Fluorescence emission was measured by fluorescence emission radiance per incident excitation irradiance ( $\text{p/sec}/\text{cm}^2/\text{sr}/\mu\text{W}/\text{cm}^2$ ).

#### 4.8. Metabolic stability

##### *Preparation of DMSO stock solutions*

A small amount ( $1.5\text{-}5 \text{ mg}$ ) of each compound was weighed in an Eppendorf cup on a XP26 Delta Range<sup>®</sup> (METTLER TOLEDO) weighing machine. An exact amount of DMSO was added to prepare the DMSO stock solutions with a defined concentration. The concentrations of the solutions were  $10 \text{ mM}$ , if not stated otherwise.

##### *Preparation of aliquots*

Aliquots of the cofactors NADPH and UDPGA were prepared by weighing an exact amount of each cofactor in an EPPENDORF cup on a XP26 Delta Range<sup>®</sup> (METTLER TOLEDO) weighing machine. They were stored at  $-20^\circ\text{C}$  prior to use and solved in an exact amount of PBS ( $0.1 \text{ M}$ ,  $\text{pH } 7.4$ ) to give the desired concentration.

##### *Preparation of mouse liver microsomes*

Deep Frozen livers ( $-80^\circ\text{C}$ ) of C57/BL6 mice were obtained from the European Institute for Molecular Imaging (Münster, Germany). Livers ( $30 \text{ g}$ ) were thawed in  $1.15 \%$  ( $\text{m}/\text{v}$ ) potassium chloride solution at  $4^\circ\text{C}$  and cut in slices and homogenized in an Elvehjem-Potter ( $10 \text{ strokes}$ ,  $3 \text{ s}$ ) with cold phosphate buffer ( $30 \text{ mL}$ ,  $\text{pH } 7.4$ ,  $0.1 \text{ M}$ ) containing sodium EDTA ( $0.5 \text{ mM}$ ). Cold sodium phosphate buffer ( $90 \text{ mL}$ ,  $\text{pH } 7.4$ ,  $0.1 \text{ M}$ ) was added

and the resulting suspension was centrifuged at 9,000 g for 20 min at 4 °C. The supernatant was centrifuged at 45,000 g for 90 min. The resulting microsome pellet was suspended in sodium phosphate buffer (pH 7.4, 0.1 M). Aliquots were stored at -80 °C prior to use.

#### *Determination of the protein concentration*

The determination of the protein concentration of the mice liver microsomes was done according to Bradford.<sup>[73]</sup> Coomassie® Brilliant Blue G 250 (5 mg) was dissolved in abs. ethanol (2.5 mL). Dist. water (10 mL) and phosphoric acid (5 mL) were added. The solution was diluted with dist. water to 50 mL. The resulting solution was stored under darkness and at 4 °C overnight. Before the experiment, the solution was filtered twice through paper filters. A stock solution of BSA in dist. water (10 mg/mL) was prepared. A multi-point calibration curve (0.05 mg/mL, 0.1 mg/mL, 0.2 mg/mL, 0.3 mg/mL, 0.4 mg/mL, 0.5 mg/mL) was performed by dilution of the stock solution with dist. water. The samples were diluted 20-fold (50 µL microsome solution, 200 µL 1 M NaOH, 750 µL dist. water) and 50-fold (20 µL microsome solution, 200 µL 1 M NaOH, 780 µL dist. water). The measurements were performed in a 96-well plate. To 10 µL of diluted sample or 10 µL of calibration solution 190 µL Bradford solution were added. The plate was shaken for 5 min and the absorption was recorded at 595 nm. Sample and calibration solutions were prepared in triplicate and measured once.

#### *Incubation procedure for 1 with mouse liver microsome suspension*

1 µL of the DMSO stock solution (10 mM) of the respective compound was added to 73 µL of PBS (pH 7.4, 0.1 M), 50 µL of magnesium chloride solution (50 mM), 26 µL of microsome suspension (mouse liver, 7.8 mg/mL protein), 50 µL NADPH solution (2 mg/mL in PBS) and 50 µL UDPGA solution (2 mg/mL in PBS). The suspension was mixed vigorously and incubated (90 min, 900 rpm, 37 °C). The incubation was stopped by addition of 400 µL of acetonitrile:methanol (1:1). The EPPENDORF cups were cooled down to 0 °C for 10 min using a water/ice bath. The precipitated proteins were separated via centrifugation (15 min, 16000 rpm, 4 °C) and the supernatant was analyzed with the LC/MS method 2. With the same procedure, the empty value (without stock solution) and the blank value (without NADPH and UDPGA) were prepared.

#### *LC/MS – method*

For the determination of exact masses and MS/MS experiments an LC system was coupled with a qTOF. HPLC-DAD: Solvent rack (SRD 3600), Pump (DGP-3600RS), Autosampler (WPS-3000RS), Column oven (TCC-3000RS), DAD-detector (DAD-3000RS) operating at 230 and 250 nm. The LC system was coupled with a microOTOF-Q II (BRUKER DALTONICS). The ESI-qTOF was operated in positive and negative ion polarity in the full scan mode ( $m/z = 70 - 700$ ) with the following settings: capillary 4500 V; end plate offset -500 V; collision cell RF 300.0 Vpp; nebulizer 2.0 bar; dry heater 200 °C; dry gas 9.0 L/min. In case of MS/MS experiments the isolation window of the first quadrupole was set to 10  $m/z$  units. The collision energy of the second quadrupole was 35 eV. Data handling and control of the system were realized with the software DataAnalysis and Hystar (BRUKER DALTONICS). The calibration of the TOF spectra was achieved by injection of 10 mM lithium formate (isopropanol:bidest. water 1:1) via a 20 µL sample loop within each LC run at 1 – 1.2 min for calibration in the range of  $m/z = 100 - 500$ . For the range of  $m/z = 500 - 1000$  sodium formate was used as the calibrant. For an injection

volume of 100 µL sample online dilution was used. Therefore a second pump with an aqueous solvent was added to the method, to dilute the solvent of the first pump in a ratio of 1:4. For online dilution, the calibration window was set at 2.0 – 2.2 min. Detailed LC/MS gradients are described in the supporting information.

#### **4.9. Microsomal stability**

##### *LC/MS method*

UPLC-UV/MS (Agilent Technologies): Precolumn: Zorbax Eclipse Plus-C18 (2.1 × 12.5 mm, 5 µm particle size), Main column: Zorbax SB-C18 (2.1 × 50 mm, 1.8 µm particle size), Degasser: 1260 HiP (G4225A), Pump: 1260 Bin Pump (G1212B), Autosampler: 1260 HiP ALS (G1367E), Column Oven: 1290 TCC (G1316C), MS-Detector: 6120 Quadrupole LC/MS (G1978B). MS Source: Multimode source.

The alignments of the capillaries from the column oven were changed, so that the six-port-valve which normally switches between two columns was used as a divert valve to protect the mass spectrometer from salts of the sample. After 2.0 min the valve was switched from “waste” to “MS-source”. At the end of a single run the valve was switched to “waste”. The Multimode source was running only in the ESI mode. The quadrupole was running in the SIM mode. The calibration of the quadrupole was achieved by injection of APCI/APPI Tuning Mix (G2432A, AGILENT TECHNOLOGIES) once a week. Detailed LC/MS gradients and further information are described in the supporting information.

##### *Optimization of fragmentor voltage and gas temperature:*

FIA was used to determine the optimum value of the gas temperature and the fragmentor voltage for each compound. For this purpose, solutions consisting of 990 µL of bidist. H<sub>2</sub>O/CH<sub>3</sub>CN 1:1 and 10 µL of the 10 mM DMSO stock solutions were prepared. 1.0 µL of each solution was injected varying the values for the fragmentor voltage or the drying gas temperature. The highest area under the curve (AUC, SIM mode) for each analyte indicated the optimum value.

##### *MS parameter:*

ESI SIM mode:  $m/z$  874 (**1**) and  $m/z$  816 (**12**), Vaporizer temperature: 200 °C, drying gas: 12 L/min, nebulizer pressure: 35 psi, VCap: 4000 V, fragmentor voltage: 150 V, drying gas temperature: 180 °C.

##### *Materials:*

1.5 mL tubes (EPPENDORF), phosphate buffered saline tabs (SIGMA ALDRICH), rat liver microsomes, methanol (Chromasolv® LC-MS grade, FLUKA), acetonitrile (LC-MS grade, FISHER SCIENTIFIC), DMSO (FISHER SCIENTIFIC), centrifuge 5427 R and thermomixer comfort (EPPENDORF),

##### *Incubation procedure of 1 for microsomal stability:*

72.5 µL PBS (pH 7.4, 0.1 M), 50 µL MgCl<sub>2</sub> solution (0.05 M) were added to an EPPENDORF cup. After adding 50 µL of the cofactor NADPH (2 mg/mL in PBS) and 1.5 µL of the 10 mM DMSO stock solution of **1** was added, the mouse liver microsomes (26 µL, 7.8 mg protein/mL) were pipetted into the cup. The suspension was mixed vigorously and incubated for different periods of time ( $t = 5, 10, 15, 30, 60, 90$  and 120 min, 900 rpm, 37°C). The incubation was stopped by addition of 400 µL of acetonitrile/methanol (1:1) containing **12** as internal standard (2 µM). The EPPENDORF cups were cooled down to 0°C for 10 min. The precipitated proteins were separated via centrifugation (15 min, 16000 rpm, 0 °C) and the supernatant was analyzed via LC/MS. With the same procedure, the empty value

(without stock solution) and the blank value (without NADPH) were prepared.

The calibration curve was obtained by the same procedure as described above, but instead of the incubation the calibration samples were quenched by addition of 400  $\mu\text{L}$  of acetonitrile/methanol (1:1) containing internal standard **12** (2  $\mu\text{M}$ ) directly after the addition of the rat liver microsomes. Different concentrations were achieved by adding 1.5  $\mu\text{L}$  of a DMSO solution, which was prediluted of the 10 mM DMSO stock solution. In this way, the final DMSO concentration and the rest of the matrix of the calibration points match with the samples. The calibration point, with a final concentration of 10  $\mu\text{M}$  (40% parent) was used as the quality control (QC), with the mistake being 1.69%.

The MS was used in SIM mode with traces  $m/z$  874 for **1** and  $m/z$  816 for **12**. For each incubation time and each calibration point three samples were prepared. The injected volume was 15  $\mu\text{L}$  and each sample and calibration point were measured in triplicate.

### Acknowledgements

Financial support by the Deutsche Forschungsgemeinschaft (DFG, collaborative research center 656 'Molecular Cardiovascular Imaging', projects B01 and Z05) is gratefully acknowledged. Compound **ISA** was prepared by Dr. Panupun Limpachayaporn and Dr. Andreas Faust and was allocated for the use in the present investigation.

### Supplementary data

Supplementary data (experimental procedures, spectroscopic data for compounds **3**, **4**, **6**, **7**, **10** and **12** and copies of the NMR spectra of all new compounds can be found, in online version, at <http://dx.doi.org/10.1016/j.bmc.2016...>

### References and notes

- Loudet, A.; Burgess, K. *Chem. Rev.* **2007**, *107*, 4891-4932.
- Kowada, T.; Maeda, H.; Kikuchi, K. *Chem. Soc. Rev.* **2015**, *44*, 4953-4972.
- Karolin, J.; Johansson, L. B. A.; Strandberg, L.; Ny, T. *J. Am. Chem. Soc.* **1994**, *116*, 7801-7806.
- Bochkov, A. Y.; Akchurin, I. O.; Dyachenko, O. A.; Traven, V. F. *Chem. Commun.* **2013**, *49*, 11653-11655.
- Yu, C.; Jiao, L.; Li, T.; Wu, Q.; Miao, W.; Wang, J.; Wei, Y.; Mu, X.; Hao, E. *Chem. Commun.* **2015**, *51*, 16852-16855.
- Liu, H.; Lu, H.; Zhou, Z.; Shimizu, S.; Li, Z.; Kobayashi, N.; Shen, Z. *Chem. Commun.* **2015**, *51*, 1713-1716.
- Gómez-Durán, C. F. A.; Esnal, I.; Valois-Escamilla, I.; Urías-Benavides, A.; Bañuelos, J.; López Arbeloa, I.; García-Moreno, I.; Peña-Cabrera, E. *Chem. Eur. J.* **2016**, *22*, 1048-1061.
- Alford, R.; Simpson, H. M.; Duberman, J.; Hill, G. C.; Ogawa, M.; Regino, C.; Kobayashi, H.; Choyke, P. L. *Mol. Imaging* **2009**, *8*, 341-354.
- Peters, C.; Billich, A.; Ghobrial, M.; Högenauer, K.; Ullrich, T.; Nussbaumer, P. *J. Org. Chem.* **2007**, *72*, 1842-1845.
- Li, Z.; Li, L.-J.; Sun, T.; Liu, L.; Xie, Z. *Dyes Pigments* **2016**, *128*, 165-169.
- Liu, J.; He, X.; Zhang, J.; He, T.; Huang, L.; Shen, J.; Li, D.; Qiu, H.; Yin, S. *Sensor Actuat B-Chem* **2015**, *208*, 538-545.
- Sen, C. P.; Shrestha, R. G.; Shrestha, L. K.; Ariga, K.; Valiyaveetil, S. *Chem. Eur. J.* **2015**, *21*, 17344-17354.
- Zhu, S.; Zhang, J.; Janjanam, J.; Vegesna, G.; Luo, F.-T.; Tiwari, A.; Liu, H. *J. Mater. Chem. B.* **2013**, *1*, 1722-1728.
- Atilgan, S.; Ozdemir, T.; Akkaya, E. U. *Org. Lett.* **2010**, *12*, 4792-4795.
- Hudnall, T. W.; Gabbai, F. P. *Chem. Commun.* **2008**, 4596-4597.
- Barba-Bon, A.; Costero, A. M.; Gil, S.; Harriman, A.; Sancenón, F. *Chem. Eur. J.* **2014**, *20*, 6339-6347.
- Xu, W.; Bai, J.; Peng, J.; Samanta, A.; Divyanshu, Chang, Y.-T. *Chem. Commun.* **2014**, *50*, 10398-10401.
- Golovkova, T. A.; Kozlov, D. V.; Neckers, D. C. *J. Org. Chem.* **2005**, *70*, 5545-5549.
- Trieflinger, C.; Rurack, K.; Daub, J. *Angew. Chem. Int. Ed.* **2005**, *44*, 2288-2291.
- Rurack, K.; Kollmannsberger, M.; Daub, J. *Angew. Chem. Int. Ed.* **2001**, *40*, 385-387.
- Amat-Guerri, F.; Liras, M.; Carrascoso, M. L.; Sastre, R. *Photochem. Photobiol.* **2003**, *77*, 577-584.
- Arbeloa, T. L.; Arbeloa, F. L.; Arbeloa, I. L.; Garcia-Moreno, I.; Costela, A.; Sastre, R.; Amat-Guerri, F. *Chem. Phys. Lett.* **1999**, *299*, 315-321.
- Boyer, J. H.; Haag, A. M.; Sathyamoorthi, G.; Soong, M.-L.; Thangaraj, K.; Pavlopoulos, T. G. *Heteroat. Chem.* **1993**, *4*, 39-49.
- Shah, M.; Thangaraj, K.; Soong, M.-L.; Wolford, L. T.; Boyer, J. H.; Politzer, I. R.; Pavlopoulos, T. G. *Heteroat. Chem.* **1990**, *1*, 389-399.
- Bergström, F.; Mikhalyov, I.; Häggelöf, P.; Wortmann, R.; Ny, T.; Johansson, L. B. Å. *J. Am. Chem. Soc.* **2001**, *124*, 196-204.
- Haugland, R. P. in *Handbook of Fluorescent Probes and Research Chemicals, Vol. 6* (Ed.: Larison, K. D.), Molecular Probes, Eugene, Oregon, **1996**, p 118.
- Tan, K.; Jaquinod, L.; Paolesse, R.; Nardis, S.; Di Natale, C.; Di Carlo, A.; Prodi, L.; Montalti, M.; Zaccaroni, N.; Smith, K. M. *Tetrahedron* **2004**, *60*, 1099-1106.
- Yee, M.-c.; Fas, S. C.; Stohlmeyer, M. M.; Wandless, T. J.; Cimprich, K. A. *J. Biol. Chem.* **2005**, *280*, 29053-29059.
- Wagner, R. W.; Lindsey, J. S. *Pure Appl. Chem.* **1996**, *68*, 1373-1380.
- Metzker, M. L. *WO 2003066812 A2*, C12Q1/68, C12P19/34, C12N, C07H21/02, C07H21/04 ed. (Ed.: Medicine, B. C. O.), USA, **2003**.
- Dziuba, D.; Jurkiewicz, P.; Cebecauer, M.; Hof, M.; Hocek, M. *Angew. Chem.* **2016**, *55*, 174-178.
- Du, G.; Huang, S.-M.; Zhai, P.; Chen, S.-B.; Hua, W.-Z.; Tan, J.-H.; Ou, T.-M.; Huang, S.-L.; Li, D.; Gu, L.-Q.; Huang, Z.-S. *Dyes Pigments* **2014**, *107*, 97-105.
- Dziuba, D.; Pohl, R.; Hocek, M.; *Bioconjug. Chem.* **2014**, *25*, 1984-1995.
- Burke, B. P.; Clemente, G. S.; Archibald, S. J. *Contrast Media Mol. Imaging* **2015**, *10*, 96-110.
- Cavins, P.; Shaohui, Z.; Akurathi, V.; Glass, T.; Packard, A. J. *Label. Compd. Rad.* **2015**, *58*, 233.
- Liu, S.; Li, D.; Zhang, Z.; Prakash, S. G. K.; Conti, P. S.; Li, Z. *Chem. Commun.* **2014**, *50*, 7371-7373.
- Liu, S.; Lin, T. P.; Li, D.; Leamer, L.; Shan, H.; Li, Z.; Gabbai, F. P.; Conti, P. S. *Theranostics* **2013**, *3*, 181-189.
- Hendricks, J. A.; Keliher, E. J.; Wan, D.; Hilderbrand, S. A.; Weissleder, R.; Mazitschek, R. *Angew. Chem. Int. Ed.* **2012**, *51*, 4603-4606.

39. Li, Z.; Lin, T.-P.; Liu, S.; Huang, C.-W.; Hudnall, T. W.; Gabbai, F. P.; Conti, P. S. *Chem. Commun.* **2011**, *47*, 9324-9326.
40. Timmer, J. C.; Salvesen, G. S. *Cell Death Differ.* **2006**, *14*, 66-72.
41. Fischer, U.; Schulze-Osthoff, K. *Cell Death Differ.* **2005**, *12*, 942-961.
42. Limpachayaporn, P.; Schäfers, M.; Haufe, G. *Future Med. Chem.* **2015**, *7*, 1173-1196.
43. Jiang, Y.; Hansen, T. V. *Bioorg. Med. Chem. Lett.* **2011**, *21*, 1626-1629.
44. Podichetty, A. K.; Wagner, S.; Faust, A.; Schäfers, M.; Schober, O.; Kopka, K.; Haufe, G. *Future Med. Chem.* **2009**, *1*, 969-989.
45. Podichetty, A. K.; Faust, A.; Kopka, K.; Wagner, S.; Schober, O.; Schäfers, M.; Haufe, G. *Bioorg. Med. Chem.* **2009**, *17*, 2680-2688.
46. Chu, W.; Rothfuss, J.; Zhou, D.; Mach, R. H. *Bioorg. Med. Chem. Lett.* **2011**, *21*, 2192-2197.
47. Limpachayaporn, P.; Riemann, B.; Kopka, K.; Schober, O.; Schäfers, M.; Haufe, G. *Eur. J. Med. Chem.* **2013**, *64*, 562-578.
48. Chu, W.; Rothfuss, J.; d'Avignon, A.; Zeng, C.; Zhou, D.; Hotchkiss, R. S.; Mach, R. H. *J. Med. Chem.* **2007**, *50*, 3751-3755.
49. Chu, W.; Rothfuss, J.; Chu, Y.; Zhou, D.; Mach, R. H.; *J. Med. Chem.* **2009**, *52*, 2188-2191.
50. Lee, D.; Long, S. A.; Murray, J. H.; Adams, J. L.; Nuttall, M. E.; Nadeau, D. P.; Kikly, K.; Winkler, J. D.; Sung, C.-M.; Ryan, M. D.; Levy, M. A.; Keller, P. M.; DeWolf, W. E. *J. Med. Chem.* **2001**, *44*, 2015-2026.
51. Chu, W.; Zhang, J.; Zeng, C.; Rothfuss, J.; Tu, Z.; Chu, Y.; Reichert, D. E.; Welch, M. J.; Mach, R. H. *J. Med. Chem.* **2005**, *48*, 7637-7647.
52. Faust, A.; Wagner, S.; Law, M. P.; Hermann, S.; Schnöckel, U.; Keul, P.; Schober, O.; Schäfers, M.; Levkau, B.; Kopka, K. *Q. J. Nucl. Med. Mol. Imaging* **2007**, *51*, 67-73.
53. Kopka, K.; Faust, A.; Keul, P.; Wagner, S.; Breyholz, H.-J.; Höltker, C.; Schober, O.; Schäfers, M.; Levkau, B. *J. Med. Chem.* **2006**, *49*, 6704-6715.
54. Zhou, D.; Chu, W.; Rothfuss, J.; Zeng, C.; Xu, J.; Jones, L.; Welch, M. J.; Mach, R. H. *Bioorg. Med. Chem. Lett.* **2006**, *16*, 5041-5046.
55. Fortt, R.; Smith, G.; Awais, R. O.; Luthra, S. K.; Aboagye, E. O. *Nucl. Med. Biol.* **2012**, *39*, 1000-1005.
56. Challapalli, A.; Kenny, L. M.; Hallett, W. A.; Kozlowski, K.; Tomasi, G.; Gudi, M.; Al-Nahhas, A.; Coombes, R. C.; Aboagye, E. O. *J. Nucl. Med.* **2013**, *54*, 1551-1556.
57. Chen, D. L.; Zhou, D.; Chu, W.; Herrbrich, P. E.; Jones, L. A.; Rothfuss, J. M.; Engle, J. T.; Geraci, M.; Welch, M. J.; Mach, R. H. *Nucl. Med. Biol.* **2009**, *36*, 651-658.
58. Nguyen, Q.-D.; Smith, G.; Glaser, M.; Perumal, M.; Årstad, E.; Aboagye, E. O. *PNAS* **2009**, *106*, 16375-16380.
59. Chen, D.; Zhou, D.; Chu, W.; Herrbrich, P.; Engle, J.; Jones, L.; Rothfuss, J.; Geraci, M.; Welch, M.; Mach, R. *J. Nucl. Med.* **2009**, *50*, 1948.
60. Chen, D. L.; Engle, J. T.; Griffin, E. A.; Miller, J. P.; Chu, W.; Zhou, D.; Mach, R. H. *Mol. Imaging Biol.* **2015**, *17*, 384-393.
61. Zhou, D.; Chu, W.; Chen, D. L.; Wang, Q.; Reichert, D. E.; Rothfuss, J.; D'Avignon, A.; Welch, M. J.; Mach, R. H. *Org. Biomol. Chem.* **2009**, *7*, 1337-1348.
62. Chen, D. L.; Zhou, D.; Chu, W.; Herrbrich, P.; Engle, J. T.; Griffin, E.; Jones, L. A.; Rothfuss, J. M.; Geraci, M.; Hotchkiss, R. S.; Mach, R. H. *Nucl. Med. Biol.* **2012**, *39*, 137-144.
63. Thukkani, A. K.; Shoghi, K. I.; Zhou, D.; Xu, J.; Chu, W.; Novak, E.; Chen, D. L.; Gropler, R. J.; Mach, R. H. *Am. J. Nucl. Med. Mol. Imaging* **2016**, *6*, 110-119.
64. del Carmen Gimenez-Lopez, M.; Räisänen, M. T.; Chamberlain, T. W.; Weber, U.; Lebedeva, M.; Rance, G. A.; Briggs, G. A. D.; Pettifor, D.; Burlakov, V.; Buck, M.; Khlobystov, A. N. *Langmuir* **2011**, *27*, 10977-10985.
65. Zhang, X.; Xiao, Y.; Qian, X. *Org. Lett.* **2008**, *10*, 29-32.
66. Meng, G.; Zheng, M.-L.; Wang, M. *Org. Prep. Proc. Int.* **2011**, *43*, 308-311.
67. Hudnall, T. W.; Lin, T.-P.; Gabbai, F. P. *J. Fluorine Chem.* **2010**, *131*, 1182-1186.
68. Paulus, A.; Desai, P.; Carney, B.; Carlucci, G.; Reiner, T.; Brand, C.; Weber, W. A. *EJNMMI Research* **2015**, *5*, 43.
69. Wiese, C.; Große-Maestrup, E.; Galla, F.; Schepmann, D.; Hiller, A.; Fischer, S.; Ludwig, F.-A.; Deuther-Conrad, W.; Donat, C. K.; Brust, P.; Büter, L.; Karst, U.; Wünsch, B. *ChemMedChem* **2016**, *11*, 2445-2458.
70. Falck, E.; Begrow, F.; Verspohl, E. J.; Wünsch, B. *J. Pharm. Biomed. Anal.* **2014**, *94*, 36-44.
71. Baumann, A.; Faust, A.; Law, M. P.; Kuhlmann, M. T.; Kopka, K.; Schäfers, M.; Karst, U. *Anal. Chem.* **2011**, *83*, 5415-5421.
72. Prante, O.; Hocke, C.; Löber, S.; Hübner, H.; Gmeiner, P.; Kuwert, T. *Nuklearmedizin* **2006**, *45*, 41-48.
73. Bradford, M. M. *Anal. Biochem.* **1976**, *72*, 248-254.